International Journal of Engineering Science 83 (2014) 99–106

Contents lists available at ScienceDirect

International Journal of Engineering Science

journal homepage: www.elsevier.com/locate/ijengsci

Shear-induced volumetric strain in CuZr metallic glass

Jian Luo [a], Yunfeng Shi [a], Catalin R. Picu [b,*]

[a] Department of Materials Science and Engineering, Rensselaer Polytechnic Institute, Troy, NY 12180, United States
[b] Department of Mechanical, Aerospace and Nuclear Engineering, Rensselaer Polytechnic Institute, Troy, NY 12180, United States

ARTICLE INFO

Article history:
Received 11 February 2014
Accepted 14 April 2014
Available online 10 May 2014

Keywords:
Free volume
Shear-induced dilatation
Metallic glass
Molecular dynamics simulation

ABSTRACT

The shear-induced volumetric strain (SIS) of a set of model CuZr metallic glasses is studied for various deformation conditions characterized by different strain rates, temperatures and applied hydrostatic stress states. The various systems considered are obtained by quenching from the melt at different cooling rates. During shear deformation at constant pressure, the material reaches a steady state in which the sample volume remains constant. It is observed that the density of the glass during steady state deformation depends on temperature, pressure and shear strain rate, and is independent of the initial state of the sample. The SIS vanishes as the temperature of the shear test reaches the glass transition temperature. The SIS can become negative under compressive pressure since the instantaneous bulk modulus is lowered by the shear flow. The results suggest that the magnitude of the SIS is related to the difference in density between samples quenched with given finite rate and a fictitious sample quenched infinitely fast.

1. Introduction

Amorphous metals and alloys were first produced in the 1960s (Klement, Willens, & Duwez, 1960) by cooling from the melt with quenching rates higher than 10^6 K/s. Since the 1990s, multi-component metallic glasses were intensively studied (Inoue, 2000). These compounds remain in the amorphous state even for cooling rates as low as 1 K/s (Li et al., 2011). This led to the proliferation of research on bulk metallic glasses. As emerging materials, metallic glasses attracted significant attention due to their unique mechanical properties (Schuh, Hufnagel, & Ramamurty, 2007). They exhibit high strength, high elastic limit (2% at the macroscopic level (Johnson & Samwer, 2005) and 5% at the nano-scale (Tian et al., 2012)), superior hardness (Inoue, 2000) and excellent wear and corrosion resistance (Inoue, 2000).

The ductility of metallic glasses is limited by shear banding (Schuh et al., 2007), which is the major plastic deformation mode in these materials. Due to the unrestricted propagation of shear bands and the nucleation of cracks in the band region, macroscopic monolithic metallic glass materials do not exhibit tensile ductility. For such macroscopic samples, ductility is achieved only in compression (Chen, Inoue, Zhang, & Sakurai, 2006; Das et al., 2005; Liu et al., 2007; Schroers & Johnson, 2004). Ductility under tension can be observed in nanoscale metallic glass samples, or under constraints (Guo et al., 2007; Jang & Greer, 2010; Luo, Wu, Huang, Wang, & Mao, 2010).

Due to the importance of shear localization in mechanical behavior of metallic glasses, significant efforts have been made to understand conditions leading to band nucleation and growth (Greer, Cheng, & Ma, 2013). The leading concept for shear band initiation is athermal softening associated with disordering of local short range ordered atomic clusters (Shi & Falk,

* Corresponding author. Tel.: +1 5182762195.
E-mail address: picuc@rpi.edu (C.R. Picu).

http://dx.doi.org/10.1016/j.ijengsci.2014.04.009
0020-7225/

2005; Shimizu, Ogata, & Li, 2006). This structural transformation is usually accompanied by free volume generation. The shear-induced volumetric strain (SIS) is also observed in other dense-packed disordered materials, including granular and colloidal assemblies (Lemaître, 2002; Schall & van Hecke, 2010). The free volume generated during shear deformation has been considered as a representative parameter for the mechanical behavior of these disordered materials (Falk & Langer, 1998; Lemaître, 2002; Spaepen, 1977).

Despite the recognized importance of the issue, the answers to several fundamental questions related to free volume production in metallic glasses remain elusive. For instance, the magnitude of SIS and its dependence on external thermomechanical loads is not entirely understood. While some calculations suggested that SIS is larger than 10% (Argon, Megusar, & Grant, 1985; Donovan & Stobbs, 1981; Megusar, Argon, & Grant, 1979; Schuh et al., 2007), recent experiment results (Klaumünzer et al., 2011; Pan, Chen, Liu, & Li, 2011) indicate that its value is limited to few percent. The difficulty of free volume evaluation during shear stems from the extreme spatial and temporal localization of deformation in the shear band. During the evolution of a shear band, the local material is far from equilibrium and has a complicated thermo-mechanical history (Lewandowski & Greer, 2005). This makes difficult the evaluation the "state" of the material in experiments. In addition, cavitation occurs preferentially in the shear band (Guan, Lu, Spector, Valavala, & Falk, 2013; Murali, Narasimhan, Guo, Zhang, & Gao, 2013; Qu, Wu, Zhang, & Eckert, 2011), which complicates the interpretation of experimental results. Therefore, further studies of SIS under well-controlled thermo-mechanical conditions are warranted. A related question is whether shear always induces dilatational hydrostatic strain, and whether compaction is possible under certain conditions. While small amplitude cyclic shear deformation is known to induce overaging, or compaction in glasses (Lacks & Osborne, 2004; Viasnoff & Lequeux, 2002), it is interesting to ask whether compaction may occur during monotonic, large strain shear deformation.

To address these issues, we perform molecular dynamics (MD) simulations of shear deformation of a model CuZr glass under a range of temperature, pressure and shear strain rate conditions. Multiple samples of same composition are produced by quenching from the melt at different cooling rates. Samples subjected to shear reach a steady flow state after yielding. The free volume increases during the transient and is constant in the steady state (SS). We discuss the parameters controlling the steady state free volume. The model and simulation methodology are presented in Section 2, the results are presented in Section 3, while conclusions are presented in closure.

2. Simulation methodology

The CuZr glass considered in this study is described by an embedded atom potential (Cheng, Ma, & Sheng, 2009) which has been validated against a large set of experimental and *ab initio* data, such as cohesive energies, enthalpies of mixing, elastic constants, etc. The potential has been used in a number of simulation studies of CuZr metallic glass (Cheng et al., 2009; Cheng & Ma, 2011; Guan, Chen, & Egami, 2010; Guan et al., 2013).

The model contains 27,000 atoms of which 50% are Cu and 50% are Zr. MD simulations are carried out using the LAMMPS package (Plimpton, 1995). The integration time-step is 1 fs. The number of atoms and the temperature are constant during each simulation. The hydrostatic stress is also kept constant and is imposed by independently controlling the normal stress in the three directions of the reference frame (Fig. 1). The Nose–Hoover equations of motion are used (Hoover, 1985; Nose, 1984) and periodic boundary conditions are applied in all directions.

The system is equilibrated for 0.1 ns in the liquid state, at 2,000 K. The glassy samples are prepared by quenching the liquid under zero pressure from the temperature of the equilibrated melt to selected lower temperatures ranging from 60 K to 1000 K. The cooling rates used are $\dot{\Theta} = 0.1$ K/ps, 0.5 K/ps, 2 K/ps, and 10 K/ps (denoted as G0.1, G0.5, G2, and G10, respectively). To explore the limit, we also generated a set of "instantly quenched" samples (denoted as G-instant) by imposing a temperature step from 2000 K to 60 K at zero pressure followed by equilibration at the lower temperature for 0.2 ns. The quenching rate in this case is dictated by the rate of response of the thermostat. The temperature stabilizes within the first 2 ps of the equilibration and hence we estimate the cooling rate for these "instantly quenched" samples to be $\dot{\Theta} \sim 1000$ K/ps.

The as-quenched samples are cubic, with the edge length of about 8 nm. This dimension varies slightly with the quenching rate and temperature. The samples are equilibrated for 20 ps at the pressure and temperature of the shear test, following which shear deformation is applied under NPT conditions. The shear strain rate is kept constant in each test and equal to 0.5 ns^{-1}, if not stated otherwise. The maximum deformation applied is 200% engineering shear strain.

3. Results and discussion

3.1. The effect of quenching rate

Let us study first the effect of quenching rate on the SIS. Samples quenched at different rates are considered and deformed in shear at zero pressure and a temperature of 60 K. Fig. 2(a) shows the variation of the volume of all samples. The starting point is the volume of the as-quenched state, which decreases as the quenching rate decreases. Upon start-up of the shear deformation, the volume increases rapidly and then gradually converges to a steady state. The volume and the applied shear

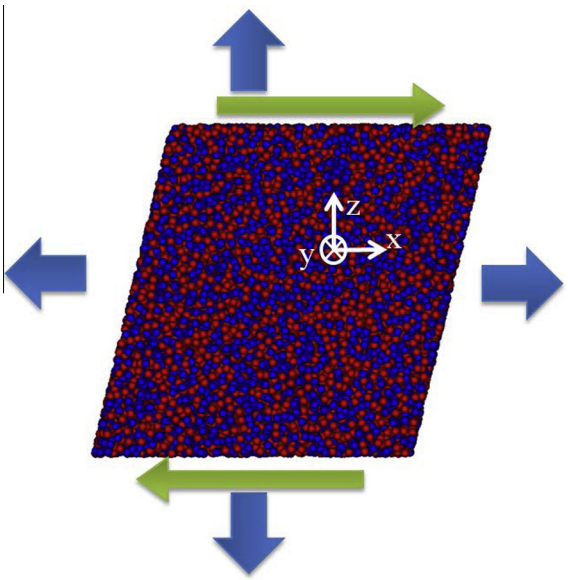

Fig. 1. Simulation cell showing a snapshot of the atomic configuration (red and blue atoms represent Zr, and Cu, respectively). Simple shear deformation is applied under isothermal-isobaric conditions. The three normal stresses are controlled independently and are kept constant and equal to each other. Periodic boundary conditions are applied in the three directions of the coordinate system.

stress become constant in SS, within the inherent (but small) atomic fluctuations. It is noted that the slowest quenched sample takes longer to reach the steady state.

In the initial phase of shear deformation, dilatation takes place heterogeneously in the sample. The shear strain is also non-uniform. As deformation proceeds, these incipient shear bands broaden and eventually engulf the entire sample. Steady state is reached at that stage. The thickness of the shear band has been shown to grow diffusively (Shi, Katz, Li, & Falk, 2007). This phenomenon is more evident in sample G0.1 which has the slowest convergence to the steady state. A similar dependence of the degree of strain localization on the quenching rate was observed before in metallic glasses (Albano & Falk, 2005; Shimizu et al., 2006).

Despite the difference between the as-quenched states, the SS of all samples overlap. The memory of the initial state is erased by the shear flow which creates a characteristic structure. This conclusion holds for the SS resulting from shear deformation applied with other strain rates and at other temperatures and pressures. As observed earlier, the flow stress is also independent of the thermo-mechanical history of the material.

Fig. 2(b) shows the volumetric strain measured from the curves in Fig. 2(a) as a function of quenching rate. The SIS effect disappears when the quenching rate is sufficiently high; specifically, the "instantly quenched" samples exhibit essentially no shear-induced volumetric change. The overall dependence of the SIS on the quenching rate is logarithmic, which is in agreement with the experimental measurement of volume relaxation over much longer time scales (Haruyama et al., 2010). The slope of the curve in Fig. 2(b), $\partial\varepsilon_{vol}/\partial log\dot{\Theta}$, is approximately 0.08%, which is slightly higher than the experimental observation of 0.03% (Haruyama et al., 2010). The magnitude of the volumetric strain is small, ranging from approximately 0 to 0.3%. Since the volumetric strain increases with decreasing $\dot{\Theta}$, we expect that these simulations provide values significantly lower than the experimental ones. The lowest quenching rate of 0.1 K/ps used here is still 10 orders of magnitude higher than common quenching rates used in experiments. With the slope measured in Fig. 2(b) it is possible to extrapolate to the experimental range of $\dot{\Theta}$. The predicted SIS for a glass quenched at $\dot{\Theta}$ = 1 K/s is 1.3%, which is in reasonable agreement with recent experimental observations by two groups reporting shear-induced dilatation strains of 1.14% (Pan et al., 2011) and approximately 2% (Klaumünzer et al., 2011), respectively.

3.2. The effect of temperature

We discuss next the effect of the temperature of the shear test on SIS. To this end, we consider samples G0.1 and G-instant and deform them at zero pressure and temperatures ranging from 60 K to 1000 K. Fig. 3(a) shows the variation of the volume of the as-quenched and SS states as a function temperature. For the G0.1 glass, the volume difference between the SS and as-quenched states (or the SIS) is noticeable at lower temperatures and decreases with increasing temperature. Therefore the SIS decreases with increasing temperature as shown in Fig. 3(b). In the case of the G-instant glass, the volumes of the as-quenched and SS states are identical; therefore, SIS is zero for all temperatures (Fig. 3(b)). Remarkably, the volume-temperature curves of the SS state for G0.1 and G-instant overlap over the entire temperature range, reinforcing the observation that the density of the SS state is quenching rate independent.

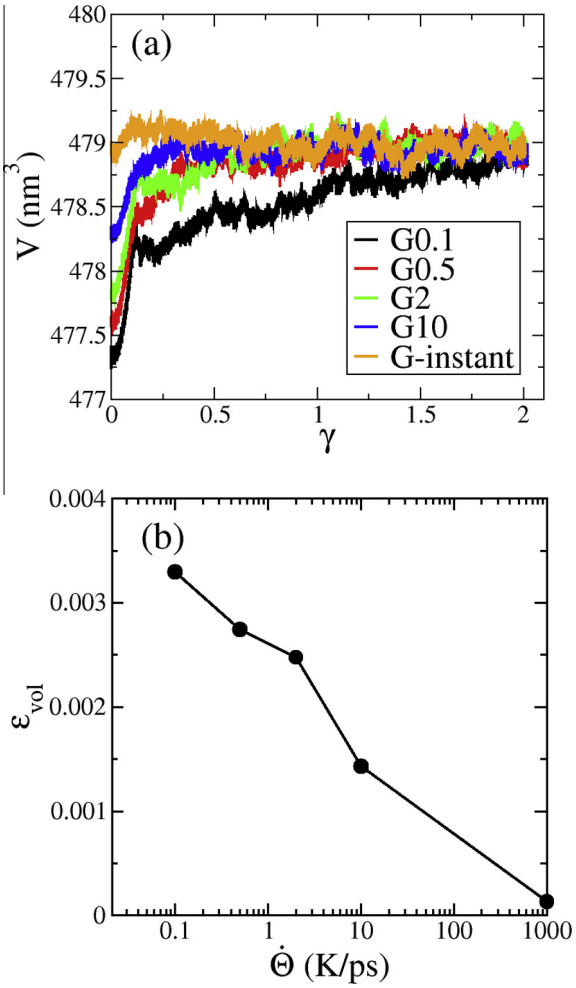

Fig. 2. (a) Evolution of sample volume during isothermal simple shear deformation under zero hydrostatic stress and at $T = 60$ K for samples quenched with various quenching rates, $\dot{\Theta}$. The shear strain rate used is 0.5 ns^{-1}. (b) Shear induced volumetric strain as a function of quenching rate.

The as-quenched state curves in Fig. 3(a) can be used to estimate the glass transition temperature to be approximately 700 K for the G0.1 sample and 900 K for G-instant. Since the SS state has the same density as the instantly quenched state (G-instant), we speculate that the glass transition temperature of G-instant defines the temperature at which the SIS vanishes for all glasses quenched with smaller $\dot{\Theta}$ (Fig. 3(b)).

3.3. The effect of strain rate

Relaxation is expected to take place dynamically during shearing. Fig. 4 shows the variation of the sample volume under SS conditions with the applied strain rate, *gamma*. It is seen that indeed, the density of the SS state increases when the shear strain rate decreases. This dynamic relaxation contributes to the reduction of the SIS effect at higher temperatures and lower strain rates (Fig. 3). However, the effect of temperature is more pronounced than that of strain rate, at least in the range of parameters accessible by MD simulations.

3.4. The effect of pressure

Hydrostatic stress is usually present in shear bands forming in bulk metallic glasses. Due to the transient nature of the shear banding process, real-time in situ measurements of the dependence of SIS on the local pressure are impossible with the current techniques. Therefore we proceed to estimate the dependence of the SIS on the applied pressure. The pressure is applied from the beginning of the equilibration stage that precedes shear deformation. Pressures in the range of −12 GPa (compressive) to 8 GPa (tensile) are considered. Fig. 5(a) and (b) show the variation of the sample volume during shear deformation under pressures of 8 GPa and -12 GPa, respectively, for all glasses considered in this study. The trends in Fig. 5(a) are

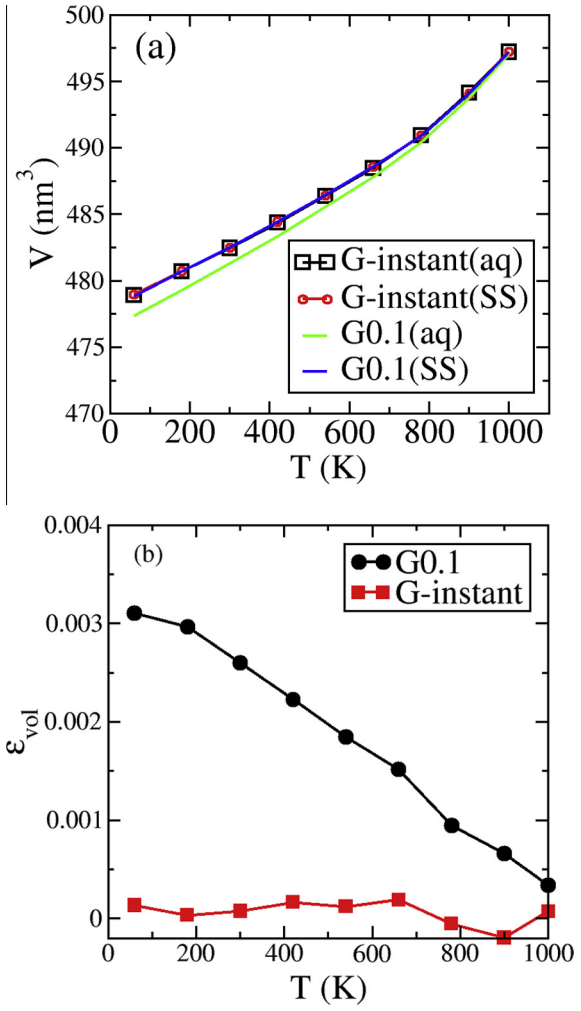

Fig. 3. (a) Variation of the volume of the as-quenched (*aq*) and steady shear (*SS*) states of G0.1 and G-instant samples with the temperature imposed during shear deformation, *T*. (b) The corresponding shear-induced volumetric strain as a function of temperature.

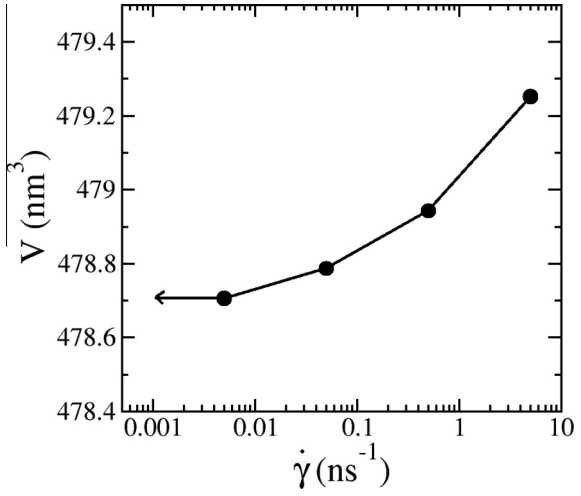

Fig. 4. Volume of the steady shear state as a function of the shear strain rate for simple shear deformations performed at zero hydrostatic stress and $T = 60$ K.

identical to those in Fig. 2(a). The density of the SS state is independent of the quenching rate under both compressive and tensile pressures. In Fig. 5(b) compaction is observed during shear. Since the pressure is constant along the entire sample trajectory, this effect can only be due to the variation of the effective bulk modulus during shearing.

Fig. 5(c) shows a schematic representation of the variation of the sample volume with the applied pressure. As the quenching rate increases, the volume of the sample in the as-quenched state increases (Figs. 2(a) and Fig. 5(a)). The volume of SS and G-instant states are identical (Fig. 2(a)). The bulk moduli of the as-quenched states are insensitive the quenching rate (Cheng & Ma, 2009; Guan et al., 2013). In our simulations, the bulk modulus of G-instant is only 1% smaller than that of G0.1, however the bulk modulus of the SS is lower than that of G0.1 by 5%. This effect is seen in Fig. 5(d) which shows the dependence of the SIS effect on the applied pressure. The slopes of these curves can be computed as:

$$\partial\varepsilon_{vol}/\partial P = \partial\left(\frac{V_{ss}-V_{aq}}{V_{aq}}\right)\Big/\partial P = \frac{V_{ss}}{V_{aq}}\left(\frac{1}{K_{ss}}-\frac{1}{K_{aq}}\right), \tag{1}$$

where V and K represent the volume and effective bulk modulus, respectively. The subscript aq and ss stand for as-quenched and steady shear states. Using the values of V_{ss} and V_{aq} from Figs. 5(a) and (b), the results in Fig. 5(d) indicate that the effective bulk modulus of SS state, K_{ss}, is smaller than that of the as-quenched state, K_{aq}.

Therefore one may write the superposition of the shear-induced dilatation strain and the volumetric strain associated with the variation of the bulk modulus during the isobaric shearing as:

$$\varepsilon_{vol}(P) = \varepsilon_{vol}(0) + \frac{V_{ss}}{V_{aq}}\left(\frac{1}{K_{ss}}-\frac{1}{K_{aq}}\right)P, \tag{2}$$

where $\varepsilon_{vol}(0)$ stands for the SIS effect, while the second term is given by Eq. (1). Note that $\varepsilon_{vol}(0)$ and V_{aq} depend on the quenching rate, while K_{ss} and V_{ss} do not since they refers to the SS state which is independent of the sample history.

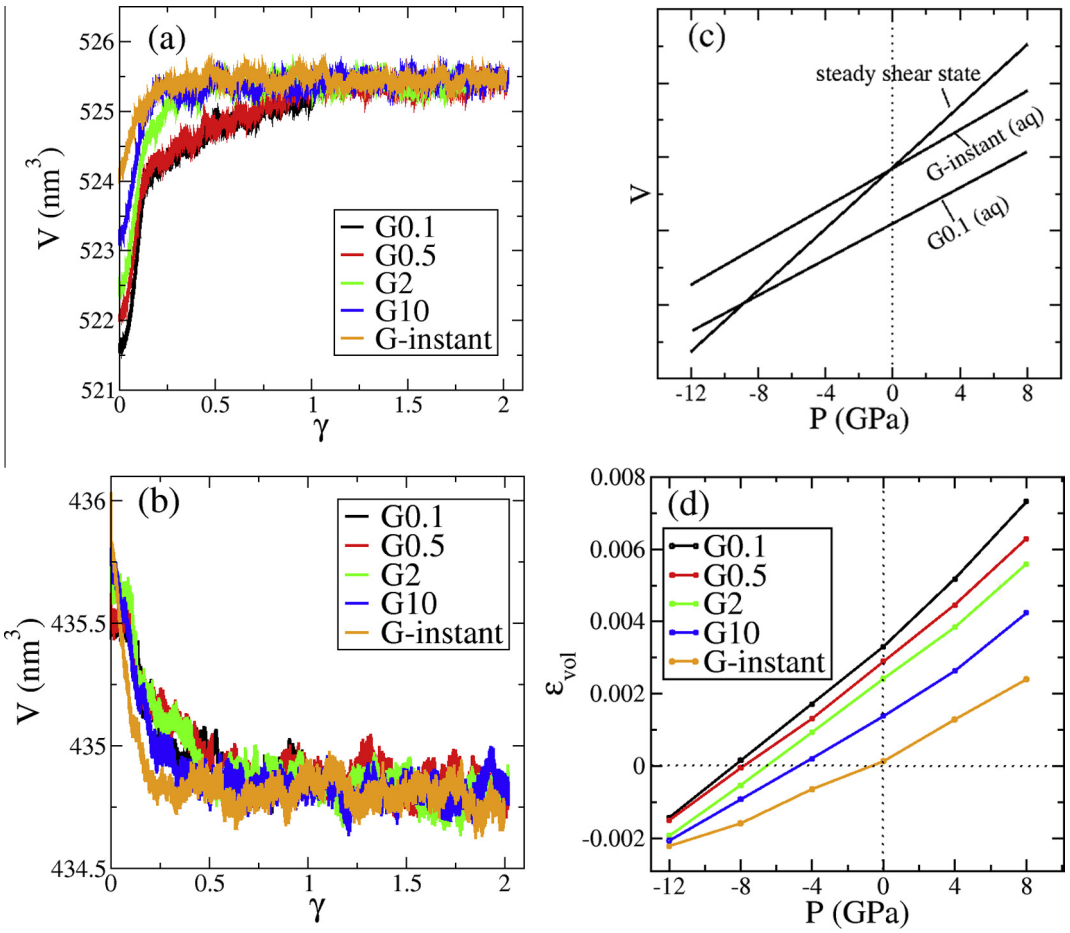

Fig. 5. Evolution of sample volume during isothermal simple shear deformation under hydrostatic pressure (a) $P = 8$ GPa and (b) $P = -12$ GPa, and at $T = 60$ K for samples quenched with various rates, $\dot{\Theta}$. The shear strain rate used is 0.5 ns^{-1}. (c) Schematic illustration of the variation of volume with pressure for the SS state and the as-quenched state of G-instant and G0.1. (d) Volumetric strain as a function of pressure, P, for samples quenched with various rates.

An interesting observation is that while the free volume content is the same in G-instant and the corresponding SS state, the effective bulk modulus is not identical, indicating that there exist subtle differences between G-instant and the SS state that do not reflect in the free volume.

4. Conclusion

In summary, the MD simulation results discussed here reveal that the SS state of the CuZr glass exhibits a density equal to that of the instantly quenched liquid over a wide temperature range under zero pressure, independent of the initial state of the glass. The SIS is a result of the rejuvenation of the aged glass state to the "instantly quenched" liquid state. Hence, SIS does not have to be dilatational if the instantly quenched liquid state possesses a higher density. Indeed, this was observed in amorphous Si in an earlier study (Argon & Demkowicz, 2008). The magnitude of SIS depends on the quenching rate, and is estimated to be on the order of few percent even for glass cooled at experimental cooling rates. This is in agreement with recent experimental results (Klaumünzer et al., 2011; Pan et al., 2011). The effective bulk modulus of the SS state is lower than that of the as-quenched state which, in turn, is also known to be independent of the quenching rate for this material system. This observation suggests that there exist subtle differences between the instantly quenched liquid and SS state that cannot be described by free volume alone.

Acknowledgment

We thank the support from the National Science Foundation (NSF) under grant DMR-1207439 and from the Center for Computational Innovations (CCI) at Rensselaer Polytechnic Institute.

References

Albano, F., & Falk, M. L. (2005). Shear softening and structure in a simulated three-dimensional binary glass. *The Journal of Chemical Physics, 122*(15), 154508. http://dx.doi.org/10.1063/1.1885000.

Argon, A. S., & Demkowicz, M. J. (2008). What can plasticity of amorphous silicon tell us about plasticity of metallic glasses? *Metallurgical and Materials Transactions A, 39*(8), 1762–1778. http://dx.doi.org/10.1007/s11661-007-9368-2.

Argon, A. S., Megusar, J., & Grant, N. J. (1985). Shear band induced dilations in metallic glasses. *Scripta Metallurgica, 19*(5), 591–596. http://dx.doi.org/10.1016/0036-9748(85)90343-6.

Chen, M., Inoue, A., Zhang, W., & Sakurai, T. (2006). Extraordinary plasticity of ductile bulk metallic glasses. *Physical Review Letters, 96*(24). http://dx.doi.org/10.1103/PhysRevLett. 96.245502.

Cheng, Y., & Ma, E. (2009). Configurational dependence of elastic modulus of metallic glass. *Physical Review B, 80*(6). http://dx.doi.org/10.1103/PhysRevB.80.064104.

Cheng, Y., Ma, E., & Sheng, H. (2009). Atomic level structure in multicomponent bulk metallic glass. *Physical Review Letters, 102*(24). http://dx.doi.org/10.1103/PhysRevLett. 102.245501.

Cheng, Y. Q., & Ma, E. (2011). Intrinsic shear strength of metallic glass. *Acta Materialia, 59*(4), 1800–1807. http://dx.doi.org/10.1016/j.actamat.2010.11.046.

Das, J., Tang, M., Kim, K., Theissmann, R., Baier, F., Wang, W., & Eckert, J. (2005). "Work-hardenable" ductile bulk metallic glass. *Physical Review Letters, 94*(20). http://dx.doi.org/10.1103/PhysRevLett. 94.205501.

Donovan, P. E., & Stobbs, W. M. (1981). The structure of shear bands in metallic glasses. *Acta Metallurgica, 29*(8), 1419–1436. http://dx.doi.org/10.1016/0001-6160(81)90177-2.

Falk, M. L., & Langer, J. S. (1998). Dynamics of viscoplastic deformation in amorphous solids. *Physical Review E, 57*(6), 7192.

Greer, A. L., Cheng, Y. Q., & Ma, E. (2013). Shear bands in metallic glasses. *Materials Science and Engineering: R: Reports, 74*(4), 71–132. http://dx.doi.org/10.1016/j.mser.2013.04.001.

Guan, P., Chen, M., & Egami, T. (2010). Stress-temperature scaling for steady-state flow in metallic glasses. *Physical Review Letters, 104*(20). http://dx.doi.org/10.1103/PhysRevLett. 104.205701.

Guan, P., Lu, S., Spector, M. J. B., Valavala, P. K., & Falk, M. L. (2013). Cavitation in amorphous solids. *Physical Review Letters, 110*(18). http://dx.doi.org/10.1103/PhysRevLett. 110.185502.

Guo, H., Yan, P. F., Wang, Y. B., Tan, J., Zhang, Z. F., Sui, M. L., & Ma, E. (2007). Tensile ductility and necking of metallic glass. *Nature Materials, 6*(10), 735–739. http://dx.doi.org/10.1038/nmat1984.

Haruyama, O., Nakayama, Y., Wada, R., Tokunaga, H., Okada, J., Ishikawa, T., & Yokoyama, Y. (2010). Volume and enthalpy relaxation in Zr55Cu30Ni5Al10 bulk metallic glass. *Acta Materialia, 58*(5), 1829–1836. http://dx.doi.org/10.1016/j.actamat.2009.11.025.

Hoover, W. G. (1985). Canonical dynamics – equilibrium phase-space distributions. *Physical Review A, 31*(3), 1695–1697.

Inoue, A. (2000). Stabilization of metallic supercooled liquid and bulk amorphous alloys. *Acta Mater, 48*(279), 306.

Jang, D., & Greer, J. R. (2010). Transition from a strong-yet-brittle to a stronger-and-ductile state by size reduction of metallic glasses. *Nature Materials*. http://dx.doi.org/10.1038/nmat2622.

Johnson, W., & Samwer, K. (2005). A universal criterion for plastic yielding of metallic glasses with a (T/Tg)2/3 temperature dependence. *Physical Review Letters, 95*(19). http://dx.doi.org/10.1103/PhysRevLett. 95.195501.

Klaumünzer, D., Lazarev, A., Maaß, R., Dalla Torre, F. H., Vinogradov, A., & Löffler, J. F. (2011). Probing shear-band initiation in metallic glasses. *Physical Review Letters, 107*(18). http://dx.doi.org/10.1103/PhysRevLett. 107.185502.

Klement, W., Willens, R. H., & Duwez, P. (1960). Non-crystalline structure in solidified gold-silicon alloys. *Nature, 187*(4740), 869–870. http://dx.doi.org/10.1038/187869b0.

Lacks, D., & Osborne, M. (2004). Energy landscape picture of overaging and rejuvenation in a sheared glass. *Physical Review Letters, 93*(25). http://dx.doi.org/10.1103/PhysRevLett. 93.255501.

Lemaître, A. (2002). Rearrangements and dilatancy for sheared dense materials. *Physical Review Letters, 89*(19). http://dx.doi.org/10.1103/PhysRevLett. 89.195503.

Lewandowski, J. J., & Greer, A. L. (2005). Temperature rise at shear bands in metallic glasses. *Nature Materials, 5*(1), 15–18. http://dx.doi.org/10.1038/nmat1536.

Li, Y., Poon, S. J., Shiflet, G. J., Xu, J., Kim, D. H., & Löffler, J. F. (2011). Formation of bulk metallic glasses and their composites. *MRS Bulletin, 32*(08), 624–628. http://dx.doi.org/10.1557/mrs2007.123.

Liu, Y. H., Wang, G., Wang, R. J., Zhao, D. Q., Pan, M. X., & Wang, W. H. (2007). Super plastic bulk metallic glasses at room temperature. *Science, 315*(5817), 1385–1388. http://dx.doi.org/10.1126/science.1136726.

Luo, J. H., Wu, F. F., Huang, J. Y., Wang, J. Q., & Mao, S. X. (2010). Superelongation and atomic chain formation in nanosized metallic glass. *Physical Review Letters, 104*(21). http://dx.doi.org/10.1103/PhysRevLett. 104.215503.
Megusar, J., Argon, A. S., & Grant, N. J. (1979). Plastic flow and fracture in Pd80Si20 near Tg. *Materials Science and Engineering, 38*(1), 63–72. http://dx.doi.org/10.1016/0025-5416(79)90033-8.
Murali, P., Narasimhan, R., Guo, T. F., Zhang, Y. W., & Gao, H. J. (2013). Shear bands mediate cavitation in brittle metallic glasses. *Scripta Materialia, 68*(8), 567–570. http://dx.doi.org/10.1016/j.scriptamat.2012.11.038.
Nose, S. (1984). A unified formulation of the constant temperature molecular-dynamics methods. *Journal of Chemical Physics, 81*(1), 511–519.
Pan, J., Chen, Q., Liu, L., & Li, Y. (2011). Softening and dilatation in a single shear band. *Acta Materialia, 59*(13), 5146–5158. http://dx.doi.org/10.1016/j.actamat.2011.04.047.
Plimpton, S. (1995). Fast parallel algorithms for short-range molecular dynamics. *Journal of Computational Physics, 117*(1), 1–19. http://dx.doi.org/10.1006/jcph.1995.1039.
Qu, R. T., Wu, F., Zhang, Z.-F., & Eckert, J. (2011). Direct observations on the evolution of shear bands into cracks in metallic glass. *Journal of Materials Research, 24*(10), 3130–3135. http://dx.doi.org/10.1557/jmr.2009.0374.
Schall, P., & van Hecke, M. (2010). Shear bands in matter with granularity. *Annual Review of Fluid Mechanics, 42*(1), 67–88. http://dx.doi.org/10.1146/annurev-fluid-121108-145544.
Schroers, J., & Johnson, W. L. (2004). Ductile bulk metallic glass. *Physical Review Letters, 93*(25), 255506.
Schuh, C., Hufnagel, T., & Ramamurty, U. (2007). Mechanical behavior of amorphous alloys. *Acta Materialia, 55*(12), 4067–4109. http://dx.doi.org/10.1016/j.actamat.2007.01.052.
Shi, Y., & Falk, M. L. (2005). Structural transformation and localization during simulated nanoindentation of a noncrystalline metal film. *Applied Physics Letters, 86*(1), 011914. http://dx.doi.org/10.1063/1.1844593.
Shi, Y., Katz, M., Li, H., & Falk, M. (2007). Evaluation of the disorder temperature and free-volume formalisms via simulations of shear banding in amorphous solids. *Physical Review Letters, 98*(18). http://dx.doi.org/10.1103/PhysRevLett. 98.185505.
Shimizu, F., Ogata, S., & Li, J. (2006). Yield point of metallic glass. *Acta Materialia, 54*(16), 4293–4298. http://dx.doi.org/10.1016/j.actamat.2006.05.024.
Spaepen, F. (1977). A microscopic mechanism for steady state inhomogeneous flow in metallic glasses. *Acta Metallurgica, 25*(4), 407–415. http://dx.doi.org/10.1016/0001-6160(77)90232-2.
Tian, L., Cheng, Y.-Q., Shan, Z.-W., Li, J., Wang, C.-C., Han, X.-D., & Ma, E. (2012). Approaching the ideal elastic limit of metallic glasses. *Nature Communications, 3*, 609. http://dx.doi.org/10.1038/ncomms1619.
Viasnoff, V., & Lequeux, F. (2002). Rejuvenation and overaging in a colloidal glass under shear. *Physical Review Letters, 89*(6). http://dx.doi.org/10.1103/PhysRevLett. 89.065701.